Research Square

Preprints are preliminary reports that have not undergone peer review.
They should not be considered conclusive, used to inform clinical practice,
or referenced by the media as validated information.

Temporal Imprecision of the Self in Early Psychosis: Abnormal Infraslow Phase Dynamics and Brain Complexity

Georg Northoff
Georg.Northoff@theroyal.ca

University of Ottawa https://orcid.org/0000-0002-5236-0951
I-Fei Chen
https://orcid.org/0009-0007-4952-4760
Yujia Ao
Yasir Catal
Chen-Chun Liu
https://orcid.org/0000-0002-9290-110X
Tzung-Jeng Hwang
Yi-Ting Lin
https://orcid.org/0000-0003-3821-4744
Ming H. Hsieh
Yi-Ling Chien
Hai-Gwo Hwu
National Taiwan University Hospital https://orcid.org/0000-0002-2582-2807
Stephan Lechner
University of Vienna https://orcid.org/0000-0001-9372-323X
Chih-Min Liu
National Taiwan University Hospital https://orcid.org/0000-0001-7016-8990

Article

Keywords:

Posted Date: April 14th, 2026

DOI: https://doi.org/10.21203/rs.3.rs-9205139/v1

License: This work is licensed under a Creative Commons Attribution 4.0 International License. Read Full License

Additional Declarations: The authors have declared there is **NO** conflict of interest to disclose

Abstract

Self-disturbance is a core feature of schizophrenia (SCZ) and may emerge during the prodromal phase. Temporal imprecision has recently been proposed as a core neural mechanism in schizophrenia, primarily demonstrated in faster EEG frequency ranges. Whether such imprecision extends to infraslow brain dynamics in functional magnetic resonance imaging (fMRI) and relates to self-disturbance in early psychosis remains unknown. Here, we examined resting-state fMRI data from drug-free early psychosis patients ($EP_{drug-free,}$ n = 31, scanned before and after medication) and 31 healthy controls (HC). Brain dynamics were quantified using sample entropy (SampEn) and instantaneous peak frequency (PF) in regions associated with different layers of self-processing (interoceptive, exteroceptive, and mental). Compared to controls, $EP_{drug-free}$ showed higher SampEn and slower mean PF with greater variability than HC, particularly in the regions of the exteroceptive self. Moreover, $EP_{drug-free}$ exhibited a decoupling between SampEn and PF, whereas HC showed strong correlations. Both SampEn and PF significantly contributed to diagnostic classification, and increased SampEn was associated with greater severity of negative, disorganized, and anxiety/depression symptoms. Together, these findings indicate abnormal infraslow brain dynamics in early psychosis, characterized by increased neural complexity and disrupted temporal organization. This temporal imprecision, particularly within the exteroceptive self, may represent a key mechanism linking altered brain dynamics to self-disturbance and psychopathology in early psychosis.

Introduction

Self-disturbance, also known as self-disorder [1–3], is increasingly recognized as a fundamental psychopathological feature in the early stages of schizophrenia (SCZ) [4–7]. Individuals with early psychosis often report nonspecific symptoms such as unusual perceptual experiences, diminished sense of agency, blurred internal-external boundaries, and social alienation, often accompanied by anxiety and depression [5, 8–11]. Although theoretical models provide insights for linking phenomenology to biology [5, 12], the neural correlates of self-disturbance remain unclear, especially in early psychosis.

Various studies have shown that that sense of self overlaps with activity in higher-order brain regions, including cortical midline structures [13–15] and the temporo-parietal junction [16–18]. Based on a recent meta-analysis, Qin et al. [19] proposed a three-layer model of the self, comprising interoceptive (inner bodily self), exteroceptive (outer bodily self), and mental (cognitive self) layers (See Methods and Fig. 1). A recent systematic review by Sabbah and Northoff [20] reported that neural abnormalities in SCZ are most consistently observed in the exteroceptive and mental layers, particularly as abnormal task-related hyperactivity.

Beyond spatial abnormalities, SCZ is also characterized by altered temporal dynamics. Entropy, quantifying irregularity in resting-state BOLD signals, provides a useful neural dynamics index [21]. Elevated entropy in SCZ reflects increased temporal irregularity and dysregulation across neural [22–26] and behavioral processes [27, 28]. Sample entropy (SampEn) is widely used due to its simplicity and reliability with short time series [29]. However, the relationship between such temporal irregularities, hierarchical self-processing, and early self-disturbance in drug-free psychosis remains unclear.

In addition to temporal irregularity, phase-based measures, such as inter-trial phase coherence (ITPC), capture another dimension of neural dynamics. Electroencephalography (EEG) studies have shown reduced phase consistency and altered synchronization in SCZ during both task and rest [30–34]. This raises the question of whether temporal imprecision exists in the infraslow range as measured in functional magnetic resonance imaging (fMRI). Although abnormal phase-based functional connectivity has been observed in SCZ [35], the phase dynamics themselves remain unexplored.

The present study aimed to investigate the temporal imprecision of neural dynamics across the three self layers in early psychosis, including both drug-free and medicated patients, as well as in healthy controls (HC). We first assessed group differences in SampEn across self layers. Based on these findings, we analyzed peak frequency (PF) to investigate dynamic phase fluctuations of brain activity. To validate the phase specificity of PF effects, we used a shuffling procedure (see Methods). Control measures such as frequency power (FP) and median frequency (MF) were included to differentiate phase dynamics from amplitude and overall frequency characteristics (see Methods). Finally, we examined within-group SampEn–PF correlations and tested whether these measures predicted clinical symptoms and early psychosis status. Based on previous studies of abnormal neural dynamics in SCZ [22, 23, 31], we hypothesized that: (1) $EP_{drug-free}$ would show higher SampEn than HC and $EP_{drug-treated}$; (2) $EP_{drug-free}$ would show aberrant PF compared to HC and $EP_{drug-treatment}$; (3) SampEn–PF correlations would differ across groups; and (4) dynamic measurements would relate to clinical symptoms and predict early psychosis status.

Methods

Participants

Thirty-one individuals with early psychosis and 31 age- and sex-matched HC were included. Patient data were drawn from the cohort described in Liu et al. [36], recruited from the outpatient psychiatry clinics at National Taiwan University Hospital. Detailed recruitment procedures, diagnostic criteria, and exclusion criteria are reported in Liu et al. [36]. All patients were drug-free at baseline: 18 antipsychotic-naïve and 13 with short-term exposure (< 12 weeks). After baseline scanning, patients received flexible-dose aripiprazole. The average time between baseline and follow-up fMRI scans was 41.48 ± 15.93 days. HCs were screened using the Chinese Diagnostic Interview for Genetic Studies [37], had no psychiatric history, and completed only the baseline scan. Ethical approval and written informed consent were obtained. Demographic and clinical data appear in Table 1. Further details are available in the supplementary materials.

Table 1
Demographic and Clinical Information

	Baseline							Follow-up Day14					Follow-up Day28		
	$EP_{drug-free}$ (n = 31)		HC (n = 31)		$EP_{drug-free}$ vs. HC			$EP_{drug-treated}$ (n = 31)		$EP_{drug-free}$ vs. $EP_{drug-treated}$			$EP_{drug-treated}$ (n = 31)		EP_{drug-} vs. $EP_{}$
	N	%	N	%	Statistic	df	p								
Sex					$\chi^2 = 0$	1	1.00								
Male	15	48	15	48											
Female	16	52	16	52											
	Mean	SD	Mean	SD	Statistic	df	p	Mean	SD	Statistic	df	p	Mean	SD	Statist
Age (years)	27.55	7.69	28.31	6.45	U = 426.50		0.45								
Education (years)	14.32	2.61	15.36	2.29	U = 372.00		0.12								
Duration of Untreated Psychosis (days)	165.61	217.16													
Aripiprazole mean dose (mg)	6.83	3.48													
Mean FD	0.18	0.09	0.19	0.10	U = 473.00		0.92						0.20	0.10	t = -1.6
Invalid scans (%)	0.06	0.05	0.05	0.02	U = 475.50		0.95						0.07	0.05	t = -1.5
PANSS Marder factors															
Delusion/hallucination	22.71	5.66						16.87	6.07	U = 400.50		< 0.001	14.80	4.03	U = 406.00
Negative symptoms	15.13	6.71						12.03	5.92	U = 231.00		< 0.001	11.48	4.74	t = 5.40
Disorganized thought	15.52	4.42						11.48	4.49	t = 4.14	30	< 0.001	10.68	3.17	t = 5.93
UHE	6.97	2.20						4.97	1.66	U = 344.50		< 0.001	4.52	1.15	U = 320.50
AD	9.55	2.36						7.39	2.74	U = 286.00		< 0.001	6.97	2.75	t = 4.87

Abbreviations: EP, early psychosis; HC, healthy controls; PANSS, Positive and Negative Syndrome Scale; FD, framewise displacement; UHE, uncontrolled host
AD, anxiety/depression.

Clinical Assessments

Clinical symptoms were assessed using the Positive and Negative Syndrome Scale (PANSS) on days 14 and 28. Scores were further organized into the five Marder factor dimensions: (1) positive symptoms (delusion/hallucination), (2) negative symptoms, (3) disorganized thought, (4) uncontrolled hostility/excitement (UHE), and anxiety/depression (AD) [38]. Details of the factor recalculation are provided in supplementary Table S1.

fMRI Data Acquisition and Preprocessing

Structural T1-weighted MPRAGE images were acquired using a 3 T MRI scanner (TIM Trio, Siemens, Erlangen, Germany) with a 32-channel phased-array head coil. Imaging parameters were as follows: TR = 2000 ms, TE = 3 ms, flip angle 9°, matrix = 256 × 192 × 208, field of view (FOV) = 256 × 192 × 208 mm^3, and voxel size was 1.0 × 1.0 × 1.0 mm^3. For resting-state functional imaging, T2*-weighted functional images were acquired using echo planar imaging (EPI) with the following parameters: TR = 2000 ms, TE = 24 ms, flip angle = 90°, matrix size = 64 × 64, FOV = 256 × 256 mm, and slice thickness = 3 mm with no slice gap. The scan time for resting-state fMRI was 6 minutes. All subjects were instructed to remain awake with their eyes closed during the scan.

Resting-state fMRI data were analyzed using the CONN toolbox Version 22a [39] implemented within Statistical Parametric Mapping (SPM12, http://www.fil.ion.ucl.ac.uk/spm/software/spm12/). Preprocessing followed the default pipeline outlined by Nieto-Castanon and Whitfield-Gabrieli [40], which included realignment, slice timing correction, outlier detection using the Artifact Detection Tools (ART), segmentation into gray matter, white matter (WM), and cerebrospinal fluid (CSF), normalization, and 6-mm full-width half-maximum (FWHM) smoothing. Potential motion outliers were identified based on head motion exceeding 2 mm or global BOLD signal intensity changes greater than 3 standard deviations [41]. During denoising, we regressed out potential confounding effects, including five principal components of WM and CSF signal noise (using aCompCor) [42], motion parameters and their first order

derivatives (12 parameters) and outlier scans. Linear detrending and a band-pass filter (0.008–0.09 Hz) were applied for sample entropy and median frequency analysis. Based on our previous study [43], we identified that peak frequency has a notable effect in the 0.01–0.03 Hz range, corresponding to slow-5 (0.01–0.027 Hz). Thus, for peak frequency and frequency power analysis, we applied a band-pass filter in the slow-5 range (0.01–0.027 Hz).

Regions of Interest (ROI) Selection Based on Three Layers of Self

Brain regions corresponding to the interoceptive, exteroceptive, and mental layers of self were selected based on our previous meta-analysis [19], which has also been used in studies on SCZ and depression [44, 45]. For each self-layer, multiple spherical ROIs with a 4-mm radius were created, each centered at the reported MNI coordinates. Detailed ROI definitions and coordinates are provided in supplementary materials (Table S2).

fMRI data analysis

Sample Entropy

SampEn is a measure of the complexity or regularity of time-series data, commonly used to understand the temporal dynamics of brain activity [21], A higher SampEn reflects greater irregularity and unpredictability in the fluctuations of brain activity, and is commonly applied in recent fMRI studies [23, 26]. The primary parameters used in the calculation of SampEn are *m*, *r* and *N*. The *m* parameter specifies the number of data points to be compared, often referred to as the window or vector of data. The *r* parameter is the tolerance threshold (also called the radius) used to determine if two vectors are similar (see Fig. 1B). The final parameter, *N*, represents the total length of the dataset (which is 180 in our study). For our calculation, we used *m* = 1 and *r* = 0.3, which falls within a reliable range reported in a previous study [29]. The formula used for SampEn is:

$$\mathrm{SampEn}\ (m, r, N) = -\ln\left(\frac{A}{B}\right)$$

where *A* is the number of template pairs of length *m* + 1 that match within tolerance *r*, and *B* is the number of template pairs of length *m* that match within the same tolerance. In other words, *A* represents the proportion of matches for patterns extended by one point beyond those counted in *B*. *A* higher SampEn value indicates lower predictability and greater signal irregularity, as patterns of length *m* + 1 are less likely to match than patterns of length *m*. The script is available at http://www.georgnorthoff.com/code.

Peak frequency

PF, or frequency sliding, reflects instantaneous oscillation frequencies over time [43, 46]. It is defined as the temporal derivative of the phase angle time series. Although PF has primarily been applied in EEG research [47–51], recent work has adapted it for fMRI data [43], which we followed here. After preprocessing the resting state fMRI data, the Hilbert transform was applied to obtain the analytic signal, from which the phase time series was extracted. The first temporal derivative of the phase time series was then computed and converted into frequency values in hertz. To reduce large spikes and negative values caused by abrupt phase jumps in the unwrapped phase, a median filter (MATLAB's medfilt function) was applied to the derivative. Due to fewer time points in fMRI data compared to EEG data, we increased the median filter order from 10 (used in EEG) to 20, which better accounts for larger phase jumps in the BOLD signal. Additionally, the first and last five phase time points were discarded to minimize edge effects. Figure 1C illustrates the PF computation steps. To assess variability, we calculated the coefficient of variation (CV = SD/mean). The script is available at http://www.georgnorthoff.com/code.

Control Analysis: Median Frequency and Frequency Power

As control analyses, we computed MF, reflecting the static distribution of spectral power, and FP, capturing amplitude-based dynamics. Detailed computation procedures are provided in the supplementary materials.

Shuffling to test the phase specificity of PF

Phase dynamics reflect meaningful temporal structures in neural activity, which is altered in SCZ [31, 34] To test whether PF differences depended on structured phase dynamics, raw BOLD time points were shuffled, disrupting phase cycle (supplementary figure S1A and S1B). Based on previous findings of temporal imprecision in SCZ [31, 32, 34], we hypothesized that group differences would disappear after shuffling.

Statistical Analysis

Statistical analyses were conducted using R version 4.5 (http://www.r-project.org) and jamovi 2.3. All variables for group comparisons, correlation, and regression analyses were standardized (z-scored). Two linear mixed-effects models (LMMs) tested interaction effects, with subject as a random factor. The first model tested the group ($EP_{drug-free}$ and HC) × ROI (interoceptive, exteroceptive, mental self) effects; the second tested medication status ($EP_{drug-free}$ and $EP_{drug-treated}$) × ROI. SampEn was treated as the primary dynamic measure, given its relevance in SCZ [22, 23, 26] and its ability to reflect both phase and amplitude neural dynamics [25, 32, 34, 52].

When the group × ROI interaction was significant, simple main effects were analyzed to identify ROIs with group differences. Multiple comparisons were controlled using Bonferroni correction. Follow-up analyses in these ROIs included PF and FP (phase- and amplitude-related dynamics) and MF (overall

frequency balance) to assess whether SampEn differences were phase- or amplitude-driven. Finally, correlation, logistic regression, and multivariate regression analyses were restricted to the ROI(s) showing significant group differences.

Correlations of dynamic measures in $EP_{drug-free,}$ $EP_{drug-treated}$ and HC

Considering that SampEn reflects both phase and amplitude properties, we examined correlations among SampEn, PF, and FP separately in the $EP_{drug-free}$, $EP_{drug-treated}$, and HC groups. To test whether these relationships depend on the temporal structure of the signals, correlations were repeated using shuffled BOLD time points, generating shuffled SampEn, PF, and FP. All p-values were corrected for multiple comparisons using the false discovery rate (FDR).

Binomial Logistic Regression Analysis: Distinction of EP $_{drug-free}$ vs HC

Binomial logistic regression analyses were conducted to evaluate whether the dynamic measures that distinguished $EP_{drug-free}$ from HC in prior analyses (SampEn and PF) could predict the group classification ($EP_{drug-free}$ vs HC). The outcome variable was diagnostic group ($EP_{drug-free}$ vs. HC), with SampEn and PF as predictors.

Multivariate Regression and Correlation Analyses: Prediction of Symptom Severity

To examine whether the predictor explained variance in symptom dimensions, a multivariate linear regression was conducted with the five PANSS Marder factor scores as dependent variables and SampEn and PF as predictors. Due to non-normality, overall model significance was assessed using 10,000 permutation tests. Model fit was evaluated by comparing the full model to an intercept-only model using Pillai's trace. Next, separate regressions were performed for each symptom dimension to identify the stronger predictor, again using permutation tests. When one predictor showed consistently stronger associations, we compared a full multivariate model (both predictors) with a reduced model (stronger predictor only) using MANOVA to assess model sufficiency. Finally, correlation analyses examined associations between predictors and symptom dimensions, with *p*-values FDR-adjusted for multiple comparisons.

Results

Abnormally High Sample Entropy in the Exteroceptive Self Regions

We first examined signal irregularity using SampEn. The first LMM revealed a significant group × ROI interaction ($F(2, 120) = 5.97$, $p = .003$), with no significant main effects of group ($F(1, 60) = 0.01$, $p = .92$) or ROI ($F(2, 120) = 0.38$, $p = .69$). Post hoc Bonferroni-corrected pairwise comparisons indicated that the $EP_{drug-free}$ exhibited significantly higher SampEn than the HC group in the exteroceptive self ROI ($t(180) = 2.51$, FWE-corrected $p = .04$). No significant group differences were found in the interoceptive self ($t(180) = -0.007$, FWE-corrected $p = 1.00$) or mental self ROIs ($t(180) = -2.32$, FWE-corrected $p = .06$). In the second model, no significant medication status × ROI interaction ($F(2, 150) = 1.49$, $p = .23$), main effect of medication status ($F(1, 150) = 0.06$, $p = .81$) or ROI ($F(2, 150) = 1.87$, $p = .16$) was observed (Fig. 2). Finally, we assessed whether differences in SampEn were associated with alterations in the power spectrum by measuring the MF (slow–fast frequency balance). No significant group differences were found between $EP_{drug-free}$ and HC, or between $EP_{drug-free}$ and $EP_{drug-treatment}$ groups. These results suggest that MF may not be as sensitive to group differences as SampEn. See Supplementary Fig. S2A for details.

Together, the findings showed increased temporal irregularity (higher SampEn) specifically in the exteroceptive self region in the $EP_{drug-free}$. Moreover, this increase occurred without corresponding changes in MF, suggesting an abnormality in the regularity of the temporal dynamics rather than a shift in the slow-fast power spectrum balance.

Abnormally Low Peak Frequency with High Variability in the Exteroceptive Self Regions

Following the significant SampEn difference in the exteroceptive self ROI, we examined phase-related measures. PF was lower in $EP_{drug-free}$ than HC ($t(60) = -3.26$, $p = .002$, Cohen's d = -0.83), with no significant difference between $EP_{drug-free}$ and $EP_{drug-treatment}$ ($t(30) = -0.63$, $p = .54$, Cohen's d = -0.11) (Fig. 3A). The CV of PF was higher in $EP_{drug-free}$ than HC ($t(60) = 2.58$, $p = .01$, Cohen's d = 0.66), with no significant difference between $EP_{drug-free}$ and $EP_{drug-treatment}$ ($t(30) = 0.20$, $p = .84$, Cohen's d = 0.04) (Fig. 3B). FP, as an amplitude-related measure, showed no significant group differences, similar to MF, suggesting PF differences were primarily phase-driven. See Supplementary Figure S2B for details. Collectively, the results indicated that in the exteroceptive self of $EP_{drug-free}$ subjects, phase-based PF was lower and more variable compared with HC, whereas amplitude-based measures (FP) showed no significant differences. This suggests that the phase components of PF may underlie the observed irregularity in EP.

Shuffling of Peak Frequency – Disrupted phase-cycle structure eliminates PF group differences

After the shuffling, which randomized the raw BOLD time points and disrupted the phase-cycle structure, group differences in PF disappeared ($U = 477.00$, $p = .97$, rank-biserial correlation = 0.007). Similarly, the CV of PF showed no significant group differences ($t(60) = -0.98$, $p = .33$, Cohen's d = -0.25) (supplementary figure S3A and S3B).

Together, these data showed that disrupting the fine-grained temporal structure, specifically the precise timing of instantaneous frequency changes across the rise, peak, fall, and trough, eliminated group differences. This highlights the importance of temporal imprecision in frequency dynamics within phase cycles for differentiating the two groups.

Correlation Between Dynamic Measures – SampEn relates to PF in HC but not in EP

In $EP_{drug-free}$, SampEn did not correlate with PF (r = 0.11, *FDR*-corrected p = .57) nor with FP (r = -0.40, *FDR*-corrected p = .06). Similarly, in EPdrug-treatment, there was no correlation between SampEn and PF (r = 0.04, *FDR*-corrected p = .81) or FP (r = -0.38, *FDR*-corrected p = .07). In contrast, HC showed significant correlations between SampEn and PF (r = 0.40, *FDR*-corrected p = .03) and FP (r = -0.48, *FDR*-corrected p = .01) (supplementary figure S4A). Given the importance of the shuffling, we also conducted the same correlations for the shuffled data. After shuffling, $EP_{drug-free}$ showed no correlation with PF (r = -0.01, *FDR*-corrected p = .96) or FP (r = 0.24, *FDR*-corrected p = .37). $EP_{drug-treatment}$ showed no correlation with PF (r = -0.05, *FDR*-corrected p = .96) or FP (r = 0.01, *FDR*-corrected p = .96). HC also showed no significant correlation with PF (ρ = 0.06, *FDR*-corrected p = .76) or FP (ρ = -0.23, *FDR*-corrected p = .41) (supplementary figure S4B).

Overall, SampEn correlated significantly with PF and FP in HC, but not in EP, indicating disrupted phase–entropy coupling in early psychosis. Shuffling eliminated all HC correlations, implying these depend on the temporal structure of phase dynamics, such as internal phase-cycle timing (supplementary figure S4B). The absence of such correlations in EP likely reflects imprecise timing of instantaneous frequencies across phase cycle components.

Logistic Regression Analysis – SampEn and PF predict EP – HC differentiation

We tested whether SampEn and PF could distinguish EP from HC using logistic regression. Overall, the model including the two significant measures (SampEn and PF) showed that the logistic regression model was a better fit to the data compared to the null model, χ^2 (2, n = 62) = 19.84, p = .002, suggesting that the model significantly distinguishes between EP and HC. The R^2 value of 0.27 (Cox and Snell) and 0.37 (Nagelkerke) suggest that the model correctly classifies 74.1% of the cases. Both measures were significant predictors: higher SampEn increased the odds of EP diagnosis (odds ratio = 2.69, 95% C. I. = 1.32, 5.49, p = .007), while higher PF was associated with a lower likelihood of EP diagnosis (odds ratio = 0.29, 95% C. I. = 0.14, 0.62, p = .001). See supplementary Table S3 for detailed statistical results.

Multivariate Regression – SampEn Predict Symptom Severity

Permutation-based multivariate regression revealed that SampEn and PF significantly predicted PANSS Marder factor scores (Pillai's trace = 0.69, F(10, 50) = 2.62, permutation p = .009). Follow-up linear regression analyses showed that SampEn significantly predicted the severity of negative symptoms, disorganized thought and AD (*FDR*-corrected p = *.02*), but not delusion/hallucination (*FDR*-corrected p = *.19*) or UHE (*FDR*-corrected p = *.83*).

In contrast, PF was not significantly associated with any of the outcome variables (*FDR*-corrected $p > .12$) (see supplementary Table S4). Given that SampEn showed stronger associations, a reduced model including only SampEn was compared to the full model using MANOVA. No significant difference was found (Pillai's trace = 0.22, F(5, 24) = 1.39, permutation p = .26), suggesting SampEn alone account for the observed effects.

Correlation Between Sample Entropy and Clinical Symptoms –Increased Entropy Relates to Higher Symptom Severity

Based on the multivariate regression results, we further used bivariate correlations between SampEn and clinical symptoms to specify the role of SampEn. The results revealed significant positive correlation between SampEn and negative symptoms (ρ = 0.59, *FDR*-corrected p = *.003*), disorganized thought (r = 0.48, *FDR*-corrected p = .01) and AD (r = 0.52, *FDR*-corrected p = .008), whereas no significant correlation with delusion/hallucination (r = 0.32, *FDR*-corrected p= .11) and UHE (r = 0.10, *FDR*-corrected p = .61) (Fig. 4).

Discussion

We demonstrate temporal imprecision in the infraslow frequency range of spontaneous brain activity in $EP_{drug-free}$, characterized by higher SampEn and slower, more variable PF. These abnormalities in the temporal structure of amplitude (SampEn) and phase (PF), especially in exteroceptive self regions, may underlie self-disturbance. These findings persisted after medication. Moreover, while SampEn and PF were correlated in HC, this relationship was disrupted in $EP_{drug-free}$. Finally, logistic regression showed that both measures predicted groups, but only SampEn correlated with symptom severity. Together, these findings highlight temporal imprecision within the exteroceptive self as a core feature of early psychosis.

Temporal imprecision I – Increased irregularity

A key finding is the elevated SampEn in the exteroceptive self of $EP_{drug-free}$ individuals, indicating increased neural complexity or disordered activity [22–26]. Previous studies report that drug-naïve or early-stage patients often show increased entropy in resting-state fMRI or EEG, potentially reflecting aberrant firing patterns and altered neural dynamics [21, 22, 24].

Our observations extend these results by showing increased entropy in the exteroceptive self. High entropy disrupt stable perceptual processing and attentional regulation, reflecting increased bottom-up sensory processing and reduced top-down inhibition [53–57]. As observed in psychedelics, elevated entropy may lead to more open cognitive states [54, 58] and a fragmented, less stable sense of self [54, 59]. Such mechanisms align with the elevated SampEn observed in the exteroceptive self, suggesting that abnormally high neural irregularity may serve as a neurophysiological marker of perceptual abnormalities in the early drug-free psychotic state – that is further supported by the close relation of SampEn to symptom severity.

Temporal imprecision II – Slower and more random phase dynamics

In addition to SampEn, $EP_{drug-free}$ showed slower and more variable PF in the exteroceptive self, specifically within the slow-5 band (0.01–0.027 Hz). Control analyses (FP, MF and shuffling) confirmed these effects are specific to phase dynamics, rather than amplitude or static frequency measures. These findings

complement findings in SCZ showing increased phase variability in the faster EEG frequency ranges (1 to 80 Hz) during both resting [32, 60] and task states [31, 34, 61]. Though tentative, the occurrence of these findings in both infraslow and faster frequency ranges suggests that temporal imprecision of phase dynamics serves as 'basic disturbance' [34].

How does PF influence input processing? Higher PF is linked to faster oscillations, increased temporal precision, and higher firing thresholds, promoting more temporally precise input selection and processing [46, 62, 63]. In contrast, lower PF reflects slower, less precise oscillations and reduced firing thresholds, increasing neuronal excitability and responsiveness to weaker inputs [46, 63, 64]. However, this heightened sensitivity may impair input filtering, making the brain more susceptible to noise, as both relevant and irrelevant inputs can trigger neural responses in a less specific way [46, 65]. Given that PF is slower and more variable indicating higher temporal imprecision, we assume that the $EP_{drug-free}$ patients are characterized by higher sensitivity to both inputs and noise as well as lower input selection – this aligns well with other findings [34, 61, 66].

Notably, the temporally imprecise and more random PF was observed primarily in the exteroceptive self, rather than the interoceptive or mental layers. This may indicate an unstable relationship of the exteroceptive self with incoming inputs, potentially reflecting reduced self-referential processing. Although not directly tested, such reduction is characteristic of basic self-disturbance in SCZ, as supported by a recent meta-analysis [20, 67]. Hence, future studies should investigate how altered phase dynamics may relate to self-referential processing under task conditions.

From brain to symptoms - Temporal imprecision across different levels

Our predictive modeling highlights the clinical implications of temporal abnormalities in neural dynamics. Logistic regression showed both SampEn and PF distinguished $EP_{drug-free}$ from HC, indicating that temporal imprecision as a potential marker of early psychosis [34]. In contrast, only SampEn correlated with symptom severity, suggesting amplitude-related temporal irregularity may more directly reflect psychosis phenomenology. This supports SampEn as a potential biomarker for symptom tracking. Previous EEG studies have shown entropy measures can distinguish SCZ from HC [22, 24]. Our findings extend this work by linking entropy in the exteroceptive self to symptoms. Group classification improved when combining SampEn and PF, highlighting the value of multiple dynamic measures. The dissociation may help distinguish EP from anxiety disorders, where entropy is also increased [68–70], but phase abnormalities such as PF alterations are not observed [34]. Hence, our findings highlight the need to consider more than just one dynamic measure in a future clinical translation.

This study has several limitations. First, although prior work reported reduced entropy after antipsychotic treatment [24], we did not observe this, possibly due to SCZ heterogeneity or treatment duration, highlighting the need for longitudinal studies. Second, entropy shows region-specific increases and decreases [71, 72], highlighting the importance of examining its spatial topography with PF. Third, analyzing PF dynamics across phase components, like rise, peak, fall, and trough may clarify mechanisms of temporal imprecision.

In conclusion, temporal imprecision, reflected by elevated entropy and slower, more variable PF, converges in the exteroceptive self of $EP_{drug-free}$. We propose a multi-level framework across different timescales in which micro-level infraslow oscillatory dynamics (0.01–0.027 Hz) shape meso-level complexity of brain signals (0.008–0.09 Hz), which in turn manifest at macro-level timescales (days to months) as psychological and psychopathological phenomena (Fig. 5). These nested temporal processes, embedded in environmental interactions, collectively characterize SCZ as a disorder of the self. By situating neural oscillations within a spatiotemporal psychopathology framework [73–75], our work connects basic neural dynamics to clinical symptoms, providing a conceptual bridge between brain and self in early psychosis.

Declarations

Financial Support

This study was supported by grants from National Science and Technology Council, Taiwan (MOST 111-2314-B-002-101-MY3) and National Taiwan University Hospital (NTUH 111-S0203; 112-S0148)

Conflicts of Interest

The authors declare no conflict of interest.

Author contributions

I.F.C. and **G.N.**: Conceptualization, Methodology. **C.M.L.**: Methodology. **C.M.L., Y.T.L., M.H.H., T.J.H., C.C.L., Y.L.C., and H.G.H.**: Data curation and Investigation. **I.F.C.**: Formal analysis, Writing – original draft and Writing – review and editing. **I.F.C., Y.A. and Y.C.**: Software and Methodology. **C.M.L., S.L.** and **G.N.**: Writing – review and editing. **C.M.L.**: Supervision, Funding acquisition.

Acknowledgments

We would like to thank all the members of the Department of Psychiatry and the staff of Department of Medical Research at National Taiwan University Hospital for their valuable administrative support. We also sincerely appreciate all the participants for their time, effort, and dedication to this study.

References

1. Northoff G. How Is Our Self Altered in Psychiatric Disorders? A Neurophenomenal Approach to Psychopathological Symptoms. Psychopathology. 2014;47(6): 365–76. https://doi.org/10.1159/000363351
2. Raballo A, Poletti M, Preti A, Parnas J. The Self in the Spectrum: A Meta-analysis of the Evidence Linking Basic Self-Disorders and Schizophrenia. Schizophr Bull. 2021;47(4): 1007–17. https://doi.org/10.1093/schbul/sbaa201
3. Sass LA, Parnas J. Schizophrenia, Consciousness, and the Self. Schizophr Bull 2003;29(3): 427–44. https://doi.org/10.1093/oxfordjournals.schbul.a007017
4. Henriksen MG, Raballo A, Nordgaard J. Self-disorders and psychopathology: a systematic review. Lancet Psychiatry. 2021;8(11): 1001–12. https://doi.org/10.1016/S2215-0366(21)00097-3
5. Mishara A, Bonoldi I, Allen P, Rutigliano G, Perez J, Fusar-Poli P, et al. Neurobiological Models of Self-Disorders in Early Schizophrenia. Schizophr Bull. 2016;42(4): 874–80. https://doi.org/10.1093/schbul/sbv123
6. Nelson B, Thompson A, Yung AR. Basic Self-Disturbance Predicts Psychosis Onset in the Ultra High Risk for Psychosis "Prodromal" Population. Schizophr Bull. 2012;38(6): 1277–87. https://doi.org/10.1093/schbul/sbs007
7. Raballo A, Monducci E, Ferrara M, Fiori Nastro P, Dario C. Developmental vulnerability to psychosis: Selective aggregation of basic self-disturbance in early onset schizophrenia. Schizophr Res. 2018;201: 367–72. https://doi.org/10.1016/j.schres.2018.05.012
8. Benrimoh D, Dlugunovych V, Wright AC, Phalen P, Funaro MC, Ferrara M, et al. On the proportion of patients who experience a prodrome prior to psychosis onset: A systematic review and meta-analysis. Mol Psychiatry. 2024;29(5):1361–81. https://doi.org/10.1038/s41380-024-02415-w
9. Cupo L, McIlwaine SV, Daneault JG, Malla AK, Iyer SN, Joober R, et al. Timing, Distribution, and Relationship Between Nonpsychotic and Subthreshold Psychotic Symptoms Prior to Emergence of a First Episode of Psychosis. Schizophr Bull. 2021;47(3): 604–14. https://doi.org/10.1093/schbul/sbaa183
10. Giersch A, Ferri F, Park S, Thompson JL, Humpston CS. Bodily Self-Disturbances and Hallucinations in Schizophrenia. Schizophr Bull. 2025;51: S241–52. https://doi.org/10.1093/schbul/sbaf063
11. Fusar-Poli P, Estradé A, Stanghellini G, Venables J, Onwumere J, Messas G, et al. The lived experience of psychosis: a bottom-up review cowritten by experts by experience and academics. World Psychiatry. 2022;21(2): 168–88. https://doi.org/10.1002/wps.20959.
12. Sass L, Feyaerts J. Self-Disorder in Schizophrenia: A Revised View (2. Theoretical Revision—Hyperreflexivity). Schizophr Bull. 2024;50(2): 472–483. https://doi.org/10.1093/schbul/sbad170
13. Qin P, Northoff G. How is our self related to midline regions and the default-mode network? Neuroimage. 2011;57(3): 1221–1233. https://doi.org/10.1016/j.neuroimage.2011.05.028
14. Northoff G, Bermpohl F. Cortical midline structures and the self. Trends Cogn Sci. 2004;8(3): 102–7. https://doi.org/10.1016/j.tics.2004.01.004
15. Sui J, Humphreys GW. The Integrative Self: How Self-Reference Integrates Perception and Memory. Trends Cogn Sci. 2015;19(12): 719–28. https://doi.org/10.1016/j.tics.2015.08.015
16. Blanke O, Arzy S. The Out-of-Body Experience: Disturbed Self-Processing at the Temporo-Parietal Junction. Neuroscientist. 2005;11(1):16–24. https://doi.org/10.1177/1073858404270885
17. Quesque F, Brass M. The role of the temporoparietal junction in self-other distinction. Brain Topogr. 2019;32(6): 943–955. https://doi.org/10.1007/s10548-019-00737-5
18. Ionta S, Heydrich L, Lenggenhager B, Mouthon M, Fornari E, Chapuis D et al. Multisensory mechanisms in temporo-parietal cortex support self-location and first-person perspective. Neuron. 2011;70(2): 363–74. https://doi.org/10.1016/j.neuron.2011.03.009
19. Qin P, Wang M, Northoff G. Linking bodily, environmental and mental states in the self—A three-level model based on a meta-analysis. Neurosci Biobehav Rev. 2020;115: 77–95. https://doi.org/10.1016/j.neubiorev.2020.05.004
20. Sabbah SG, Northoff G. Global neural self-disturbance in schizophrenia: A systematic fMRI review. Schizophr Res. 2024;269: 163–73. https://doi.org/10.1016/j.schres.2024.05.015
21. Fernández A, Gómez C, Hornero R, López-Ibor JJ. Complexity and schizophrenia. Prog Neuropsychopharmacol Biol Psychiatry. 2012;45: 267–76. https://doi.org/10.1016/j.pnpbp.2012.03.015
22. Murphy M, Stickgold R, Öngür D. Electroencephalogram Microstate Abnormalities in Early-Course Psychosis. Biol Psychiatry. Cogn Neurosci Neuroimaging. 2020;5(1): 35–44. https://doi.org/10.1016/j.bpsc.2019.07.006
23. Sokunbi MO, Gradin VB, Waiter GD, Cameron GG, Ahearn TS, Murray AD, et al. Nonlinear Complexity Analysis of Brain fMRI Signals in Schizophrenia. PLoS ONE. 2014;9(5): e95146. doi:10.1371/journal.pone.0095146
24. Takahashi T, Cho RY, Mizuno T, Kikuchi M, Murata T, Takahashi K, et al. Antipsychotics reverse abnormal EEG complexity in drug-naive schizophrenia: A multiscale entropy analysis. NeuroImage. 2010;51(1):173–82. https://doi.org/10.1016/j.neuroimage.2010.02.009
25. Wolfson EJ, Fekete T, Loewenstein Y, Shriki O. Multi-scale entropy assessment of magnetoencephalography signals in schizophrenia. Sci Rep. 2024;14(1): 14680. https://doi.org/10.1038/s41598-024-64704-2
26. Jia Y, Gu H. Identifying nonlinear dynamics of brain functional networks of patients with schizophrenia by sample entropy. Nonlinear Dyn. 2019; 96(4):2327–40. https://doi.org/10.1007/s11071-019-04924-8
27. Hauge ER, Berle JØ, Oedegaard KJ, Holsten F, Fasmer OB. Nonlinear Analysis of Motor Activity Shows Differences between Schizophrenia and Depression: A Study Using Fourier Analysis and Sample Entropy. PLoS ONE. 2011;6(1): e16291. https://doi.org/10.1371/journal.pone.0016291

28. Paulus MP, Perry W, Braff DL. The nonlinear, complex sequential organization of behavior in schizophrenic patients: neurocognitive strategies and clinical correlations. Biol Psychiatry. 1999;46(5): 662–70. https://doi.org/10.1016/S0006-3223(99)00086-4
29. Yang AC, Tsai SJ, Lin CP, Peng CK. A Strategy to Reduce Bias of Entropy Estimates in Resting-State fMRI Signals. Front Neurosci. 2018;12: 398. https://doi.org/10.3389/fnins.2018.00398
30. Koshiyama D, Kirihara K, Tada M, Nagai T, Fujioka M, Ichikawa E, et al. Electrophysiological evidence for abnormal glutamate-GABA association following psychosis onset. Transl Psychiatry. 2018;8(1): 211. https://doi.org/10.1038/s41398-018-0261-0
31. Lechner S, Hsieh MH, Lin YT, Liu CM, Chen IF, Liu CC, et al. Temporal imprecision and its dynamics in schizophrenia. Transl Psychiatry. 2025;15(1): 279. https://doi.org/10.1038/s41398-025-03510-4
32. Lechner S, Northoff G. Temporal imprecision and phase instability in schizophrenia resting state EEG. Asian J Psychiatr. 2023;86:103654. https://doi.org/10.1016/j.ajp.2023.103654
33. Valt C, Quarto T, Tavella A, Romanelli F, Fazio L, Arcara G, et al. Reduced magnetic mismatch negativity: a shared deficit in psychosis and related risk. Psychol Med. 2023;53(13): 6037–45. https://doi.org/10.1017/S003329172200321X
34. Wolff A, Northoff G. Temporal imprecision of phase coherence in schizophrenia and psychosis—dynamic mechanisms and diagnostic marker. Mol Psychiatry. 2024;29(2):425–38. https://doi.org/10.1038/s41380-023-02337-z
35. Sheng D, Pu W, Linli Z, Tian GL, Guo S, Fei Y. Aberrant global and local dynamic properties in schizophrenia with instantaneous phase method based on Hilbert transform. Psychol Med. 2023;53(5): 2125–35. https://doi.org/10.1017/S0033291721003895
36. Liu CM, Liu CC, Hsieh MH, Hwang TJ, Lin YT, Chien YL, et al. The plasma level of complement component 4A decreases with aripiprazole treatment in patients with early psychosis. Psychiatry Res. 2022;316: 114775. https://doi.org/10.1016/j.psychres.2022.114775
37. Chen WJ, Liu SK, Chang CJ, Lien YJ, Chang YH, Hwu HG. Sustained Attention Deficit and Schizotypal Personality Features in Nonpsychotic Relatives of Schizophrenic Patients. Am J Psychiatry. 1998;155(9):1214–20. https://doi.org/10.1176/ajp.155.9.1214
38. Marder SR, Davis JM, Chouinard G. The Effects of Risperidone on the Five Dimensions of Schizophrenia Derived by Factor Analysis: Combined Results of the North American Trials. J Clin Psychiatry. 1997;58(12): 538–46. https://doi.org/10.4088/JCP.v58n1205
39. Whitfield-Gabrieli S, Nieto-Castanon A. Conn: A Functional Connectivity Toolbox for Correlated and Anticorrelated Brain Networks. Brain Connect. 2012;2(3): 125–41. https://doi.org/10.1089/brain.2012.0073
40. Nieto-Castanon A, Whitfield-Gabrieli S. CONN functional connectivity toolbox: RRID SCR_009550, release 22. 22nd ed. Hilbert Press; 2022. https://doi.org/10.56441/hilbertpress.2246.5840.
41. Ferri J, Ford JM, Roach BJ, Turner JA, Van Erp TG, Voyvodic J, et al. Resting-state thalamic dysconnectivity in schizophrenia and relationships with symptoms. Psychol Med. 2018;48(15): 2492–9. https://doi.org/10.1017/S003329171800003X
42. Behzadi Y, Restom K, Liau J, Liu TT. A component based noise correction method (CompCor) for BOLD and perfusion based fMRI. NeuroImage. 2007;37(1): 90–101. https://doi.org/10.1016/j.neuroimage.2007.04.042
43. Ao Y, Catal Y, Lechner S, Hua J, Northoff G. Intrinsic neural timescales relate to the dynamics of infraslow neural waves. NeuroImage. 2024;285: 120482. https://doi.org/10.1016/j.neuroimage.2023.120482
44. Djimbouon F, Klar P, Northoff G. Shorter and inflexible intrinsic neural timescales of the self in schizophrenia. J Psychiatry Neurosci. 2025;50(1): E57–66. https://doi.org/10.1503/jpn.240093
45. Keskin K, Eker MÇ, Gönül AS, Northoff G. Abnormal global signal topography of self modulates emotion dysregulation in major depressive disorder. Transl Psychiatry. 2023;13(1): 107. https://doi.org/10.1038/s41398-023-02398-2
46. Cohen MX. Fluctuations in Oscillation Frequency Control Spike Timing and Coordinate Neural Networks. J Neurosci. 2014;34(27): 8988–98. https://doi.org/10.1523/JNEUROSCI.0261-14.2014
47. Buergers S, Noppeney U. The role of alpha oscillations in temporal binding within and across the senses. Nat Hum Behav. 2022;6(5): 732–42. https://doi.org/10.1038/s41562-022-01294-x
48. Hua J, Wolff A, Zhang J, Yao L, Zang Y, Luo J, et al. Alpha and theta peak frequency track on- and off-thoughts. Commun Biol. 2022;5(1): 209. https://doi.org/10.1038/s42003-022-03146-w
49. Rosso M, Moens B, Leman M, Moumdjian L. Neural entrainment underpins sensorimotor synchronization to dynamic rhythmic stimuli. NeuroImage. 2023;277: 120226. https://doi.org/10.1016/j.neuroimage.2023.120226
50. Samaha J, Postle BR. The Speed of Alpha-Band Oscillations Predicts the Temporal Resolution of Visual Perception. Curr Biol. 2015;25(22): 2985–90. doi:10.1016/j.cub.2015.10.007
51. Wolff A, De La Salle S, Sorgini A, Lynn E, Blier P, Knott V, et al. Atypical Temporal Dynamics of Resting State Shapes Stimulus-Evoked Activity in Depression—An EEG Study on Rest–Stimulus Interaction. Front Psychiatry. 2019;10: 719. https://doi.org/10.3389/fpsyt.2019.00719
52. Miskovic V, MacDonald KJ, Rhodes LJ, Cote KA. Changes in EEG multiscale entropy and power-law frequency scaling during the human sleep cycle. Hum Brain Mapp. 2019;40(2): 538–51. https://doi.org/10.1002/hbm.24393
53. Carhart-Harris RL. The entropic brain - revisited. Neuropharmacology. 2018;142: 167–78. https://doi.org/10.1016/j.neuropharm.2018.03.010
54. Carhart-Harris RL, Friston KJ. REBUS and the Anarchic Brain: Toward a Unified Model of the Brain Action of Psychedelics. Pharmacol Rev. 2019;71(3): 316–44. https://doi.org/10.1124/pr.118.017160
55. Cieri F, Zhuang X, Caldwell JZK, Cordes D. Brain Entropy During Aging Through a Free Energy Principle Approach. Front Hum Neurosci. 2021;15: 647513. https://doi.org/10.3389/fnhum.2021.647513

56. Cofré R, Destexhe A. Entropy and Complexity Tools Across Scales in Neuroscience: A Review. Entropy. 2025;27(2): 115. https://doi.org/10.3390/e27020115
57. Mateos DM, Guevara Erra R, Wennberg R, Perez Velazquez JL. Measures of entropy and complexity in altered states of consciousness. Cogn Neurodyn. 2018;12(1): 73–84. https://doi.org/10.1007/s11571-017-9459-8
58. Carhart-Harris RL, Leech R, Hellyer PJ, Shanahan M, Feilding A, Tagliazucchi E, et al. The entropic brain: a theory of conscious states informed by neuroimaging research with psychedelic drugs. Front Hum Neurosci. 2014;8. https://doi.org/10.3389/fnhum.2014.00020
59. Northoff G, Buccellato A, Ventura B. The Default Mode Network and inner time consciousness. Curr Opin Behav Sci. 2025;63: 101524. https://doi.org/10.1016/j.cobeha.2025.101524
60. Koshiyama D, Miyakoshi M, Tanaka-Koshiyama K, Joshi YB, Sprock J, Braff DL, et al. Abnormal phase discontinuity of alpha- and theta-frequency oscillations in schizophrenia. Schizophr Res. 2021;231: 73–81. https://doi.org/10.1016/j.schres.2021.03.007
61. Wolff A, Gomez-Pilar J, Zhang J, Choueiry J, De La Salle S, Knott V, et al. It's in the timing: reduced temporal precision in neural activity of schizophrenia. Cereb Cortex. 2022;32(16): 3441–56. https://doi.org/10.1093/cercor/bhab425
62. Hirano Y, Uhlhaas PJ. Current findings and perspectives on aberrant neural oscillations in schizophrenia. Psychiatry Clin Neurosci. 2021;75(12): 358–68. https://doi.org/10.1111/pcn.13300
63. Wang XJ. Neurophysiological and Computational Principles of Cortical Rhythms in Cognition. Physiol Rev. 2010;90(3): 1195–268. https://doi.org/10.1152/physrev.00035.2008
64. Buzsáki G, Wang XJ. Mechanisms of Gamma Oscillations. Annu Rev Neurosci. 2012;35(1): 203–25. https://doi.org/10.1146/annurev-neuro-062111-150444
65. Wolff A, De La Salle S, Sorgini A, Lynn E, Blier P, Knott V, et al. Atypical Temporal Dynamics of Resting State Shapes Stimulus-Evoked Activity in Depression—An EEG Study on Rest–Stimulus Interaction. Front Psychiatry. 2019;10: 719. https://doi.org/10.3389/fpsyt.2019.00719
66. Garrett DD, Samanez-Larkin GR, MacDonald SWS, Lindenberger U, McIntosh AR, Grady CL. Moment-to-moment brain signal variability: A next frontier in human brain mapping? Neurosci Biobehav Rev. 2013;37(4): 610–24. https://doi.org/10.1016/j.neubiorev.2013.02.015
67. Sabbah SG, Northoff G. The self in depression and anxiety as a transdiagnostic and differential-diagnostic neural marker: A systematic review. Neurosci Biobehav Rev. 2025;169: 106034. https://doi.org/10.1016/j.neubiorev.2025.106034
68. Fan S, Yu Y, Wu Y, Kai Y, Wang H, Chen Y, et al. Altered brain entropy and functional connectivity patterns in generalized anxiety disorder patients. J Affect Disord. 2023;332: 168–75. https://doi.org/10.1016/j.jad.2023.03.062
69. Grieder M, Denier N, Jann K, Strik W, Soravia LM, Adorjan K, et al. 7 tesla multiscale entropy analysis reveals increased resting-state complexity in key regions for fear and anxiety in spider-fearful individuals. NeuroImage. 2025;318: 121371. https://doi.org/10.1016/j.neuroimage.2025.121371
70. Wang Y, Wang X, Ye L, Yang Q, Cui Q, He Z, et al. Spatial complexity of brain signal is altered in patients with generalized anxiety disorder. J Affect Disord. 2019;246: 387–93. https://doi.org/10.1016/j.jad.2018.12.107
71. Liu L, Li Z, Kong D, Huang Y, Wu D, Zhao H, et al. Neuroimaging markers of aberrant brain activity and treatment response in schizophrenia patients based on brain complexity. Transl Psychiatry. 2024;14(1): 365. https://doi.org/10.1038/s41398-024-03067-8
72. Yang AC, Hong C, Liou Y, Huang K, Huang C, Liu M, et al. Decreased resting-state brain activity complexity in schizophrenia characterized by both increased regularity and randomness. Hum Brain Mapp. 2015;36(6): 2174–86. https://doi.org/10.1002/hbm.22763
73. Northoff G. Spatiotemporal Psychopathology II: How does a psychopathology of the brain's resting state look like? Spatiotemporal approach and the history of psychopathology. J Affect Disord. 2016;190: 867–79. https://doi.org/10.1016/j.jad.2015.05.008
74. Northoff G, Duncan NW. How do abnormalities in the brain's spontaneous activity translate into symptoms in schizophrenia? From an overview of resting state activity findings to a proposed spatiotemporal psychopathology. Prog Neurobiol. 2016;145–146: 26–45. https://doi.org/10.1016/j.pneurobio.2016.08.003
75. Northoff G, Hirjak D. Integrating subjective and objective—spatiotemporal approach to psychiatric disorders. Mol Psychiatry. 2023;28(10): 4022–4. https://doi.org/10.1038/s41380-023-02100-4

Figures

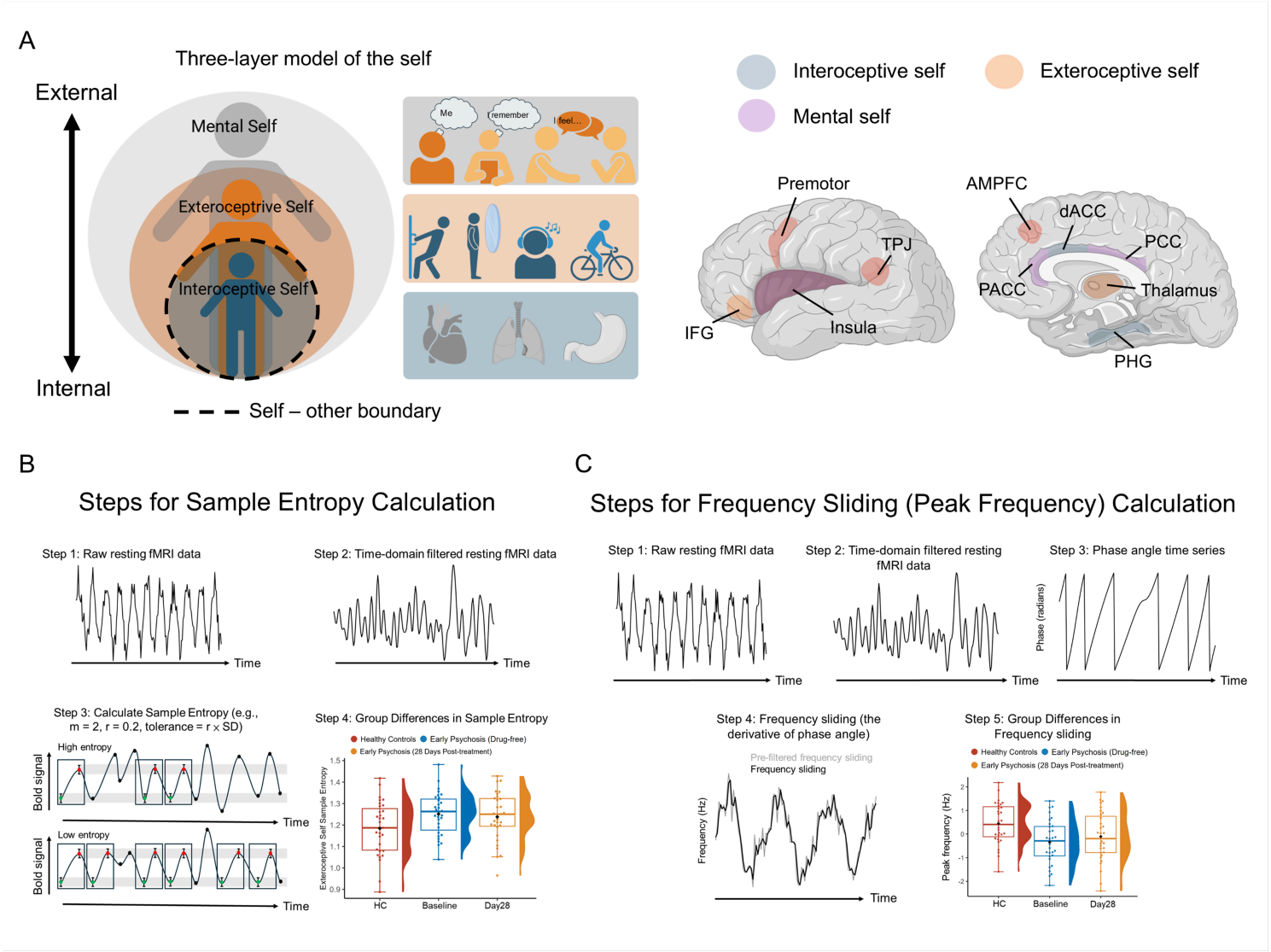


Figure 1

The three-layer model of the self and how to quantify dynamic properties of its BOLD signal. (A) The three-layer model of the self. This nested hierarchy includes three levels of self-processing: the interoceptive self (blue), the exteroceptive self (orange), and the mental self (gray). The left panel illustrates the model structure; the middle panel shows how these layers interact with the body and environment at different levels; the right panel shows the corresponding nested organization of self-related brain regions. (B) Schema of four steps for analyzing sample entropy in resting-state fMRI. Step 1: Start with raw BOLD fMRI resting-state data. Step 2: Preprocess and bandpass filter the data within 0.008–0.09 Hz. Step 3: Calculate sample entropy using parameters *m* and *r* (e.g., *m*= 2, *r* = 0.2). The diagram illustrates example signals with low and high sample entropy. Step 4: Conduct statistical group comparisons of sample entropy. (C) Schema of five steps for analyzing frequency sliding (FS), defined as temporal fluctuations in the peak oscillation frequency across the three layers of self. Step 1: Start with raw BOLD fMRI resting-state signal data. Step 2: Preprocess and bandpass filter the fMRI data into frequency bands: slow-5 (0.01–0.027 Hz). Step 3: Extract the phase angle time series by computing the analytic signal using the Hilbert transform. Step 4: Compute the temporal derivative of the phase angle time series to obtain instantaneous frequency (i.e., frequency sliding or peak frequency, PF) at each time point. Step 5: Perform statistical group comparisons of PF across the four phases. AMPFC, anteromedial prefrontal cortex; dACC, dorsal anterior cingulate cortex; pACC: pregenual anterior cingulate cortex; IFG, inferior frontal gyrus; PCC, posterior cingulate cortex; PHG, parahippocampal gyrus; Premotor, premotor cortex; TPJ, temporal parietal junction; HC, Healthy Controls; Baseline, Early Psychosis (Drug-free); Day 28, Early Psychosis (28 Days Post-treatment).

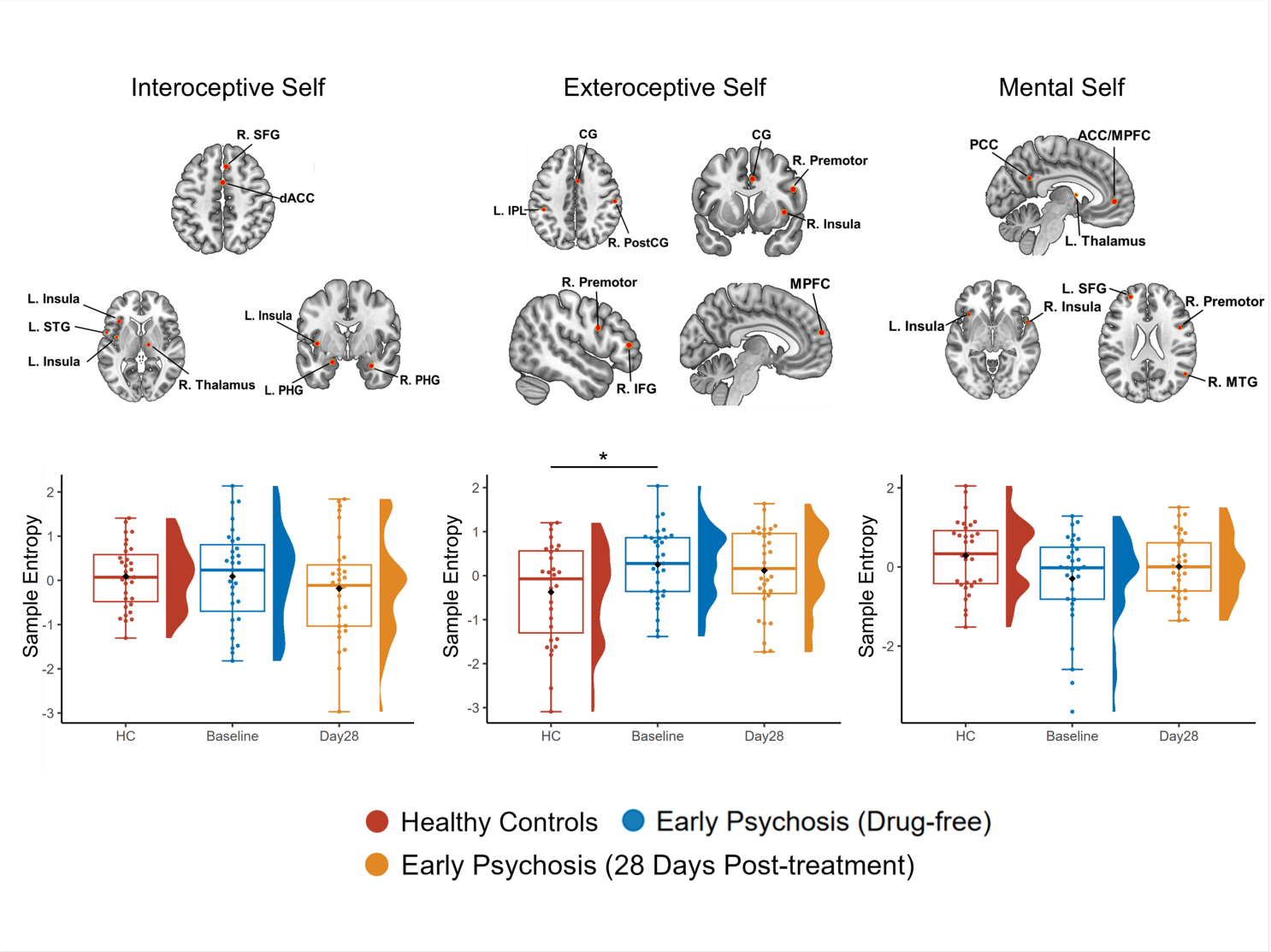


Figure 2

Group differences in Sample entropy. The upper panel shows ROIs of self-related brain regions based on Qin et al. (2020). At baseline, patients exhibited higher sample entropy in the exteroceptive self compared to HC shown in the lower panel. Results were thresholded at FWE-corrected $p < .05$. Baseline, Early Psychosis (Drug-free); HC, Healthy Controls; Day 28, Early Psychosis (28 Days Post-treatment); ACC, anterior cingulate cortex; dACC, dorsal anterior cingulate cortex; CG, cingulate gyrus; IFG, inferior frontal gyrus; IPL, inferior parietal lobule; MPFC, medial prefrontal cortex; MTG, middle temporal gyrus; PCC, posterior cingulate cortex; PHG, parahippocampal gyrus; PostCG, postcentral gyrus; Premotor, premotor cortex; SFG, superior frontal gyrus; STG, superior temporal gyrus; L., left; R., right.

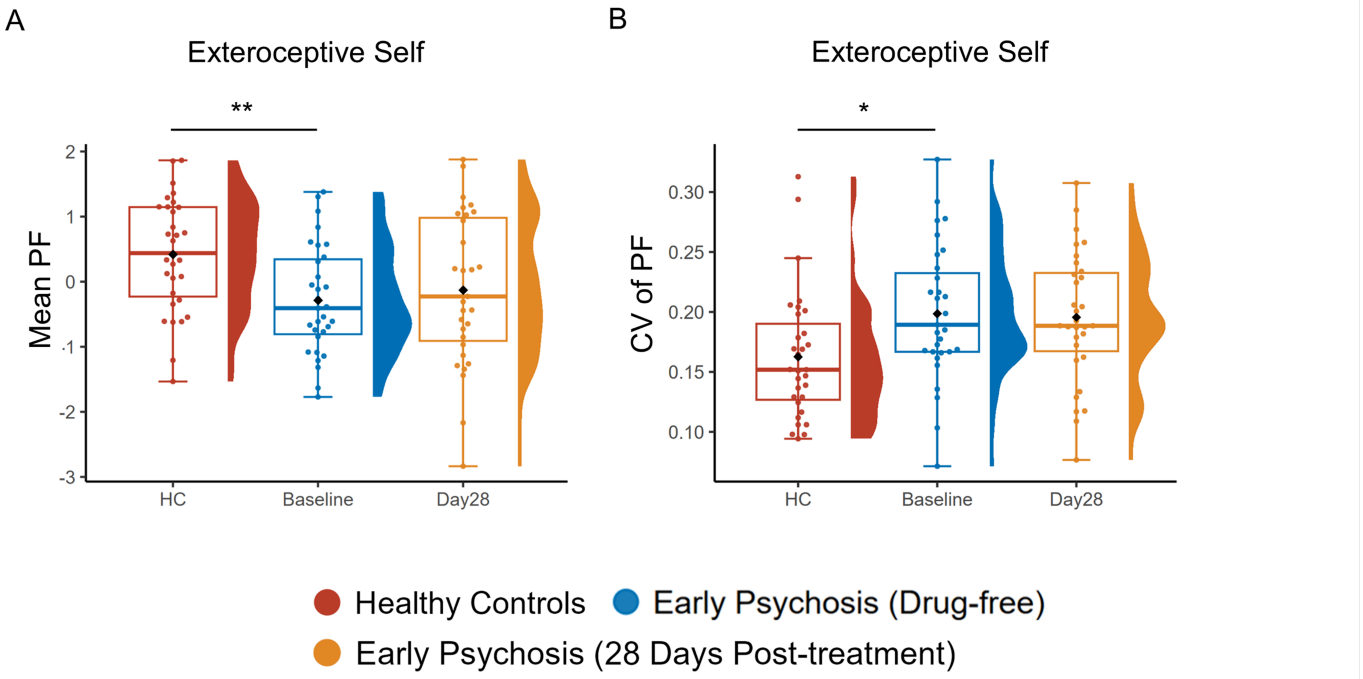


Figure 3

Group differences in peak frequency. (A) At baseline, patients showed lower PF in the exteroceptive self compared to HC. (B) At baseline, patients showed higher CV of PF than HC in the exteroceptive self. CV, coefficient of variation; Baseline, Early Psychosis (Drug-free); HC, Healthy Controls; Day 28, Early Psychosis (28 Days Post-treatment); PF, peak frequency.

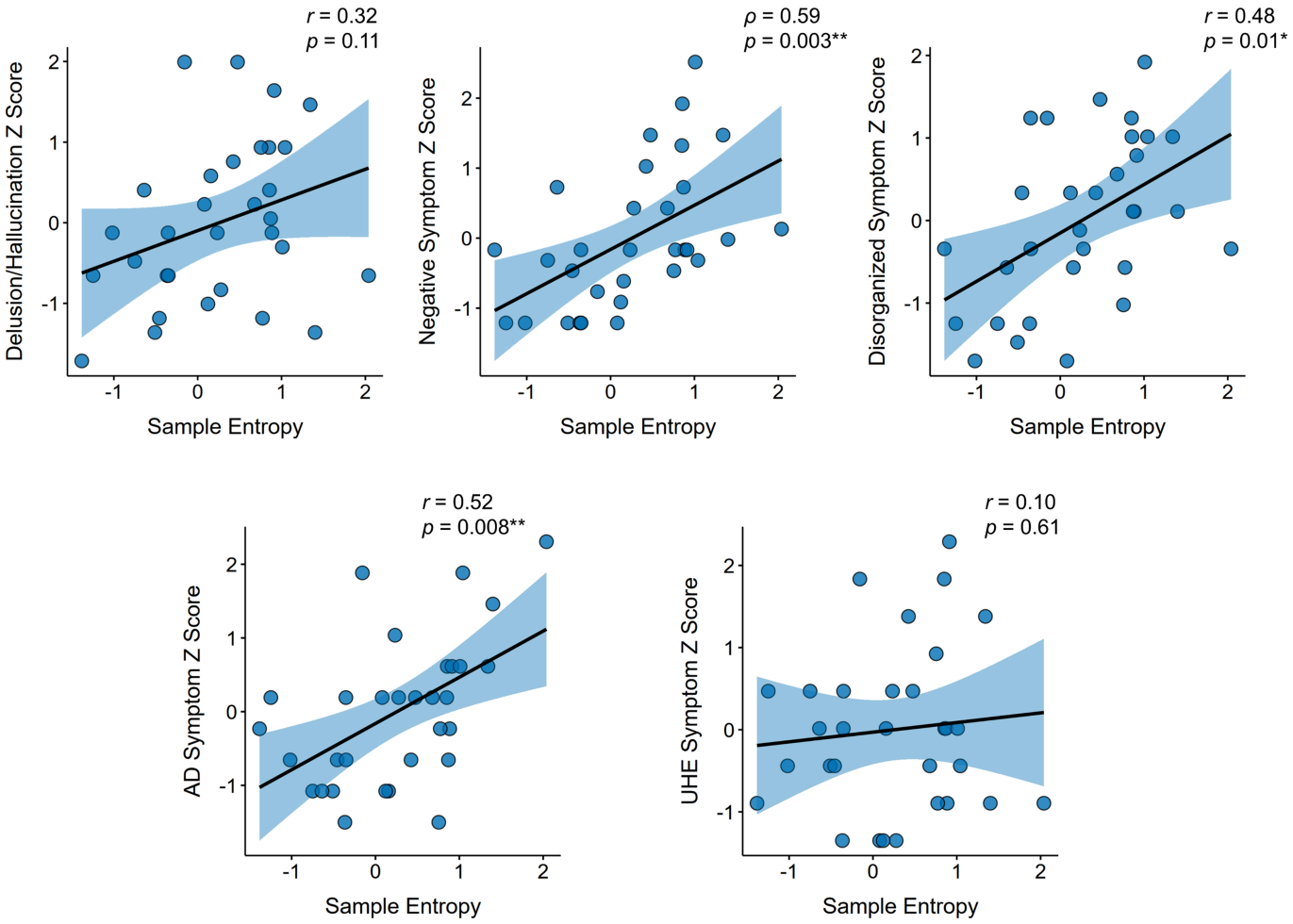


Figure 4

Correlation between sample entropy and clinical symptoms. At baseline, in patients, sample entropy was positively correlated with negative symptoms, disorganized symptoms, and AD. No significant correlations were observed with delusion/hallucination or UHE. All adjusted *p*-values were FDR-corrected. *indicates significance at adjusted p < .05. ** indicates significance at adjusted p < .01. *r* = Pearson correlation; *ρ*= Spearman's rho; AD = anxiety/depression; UHE = uncontrolled hostility/excitement.

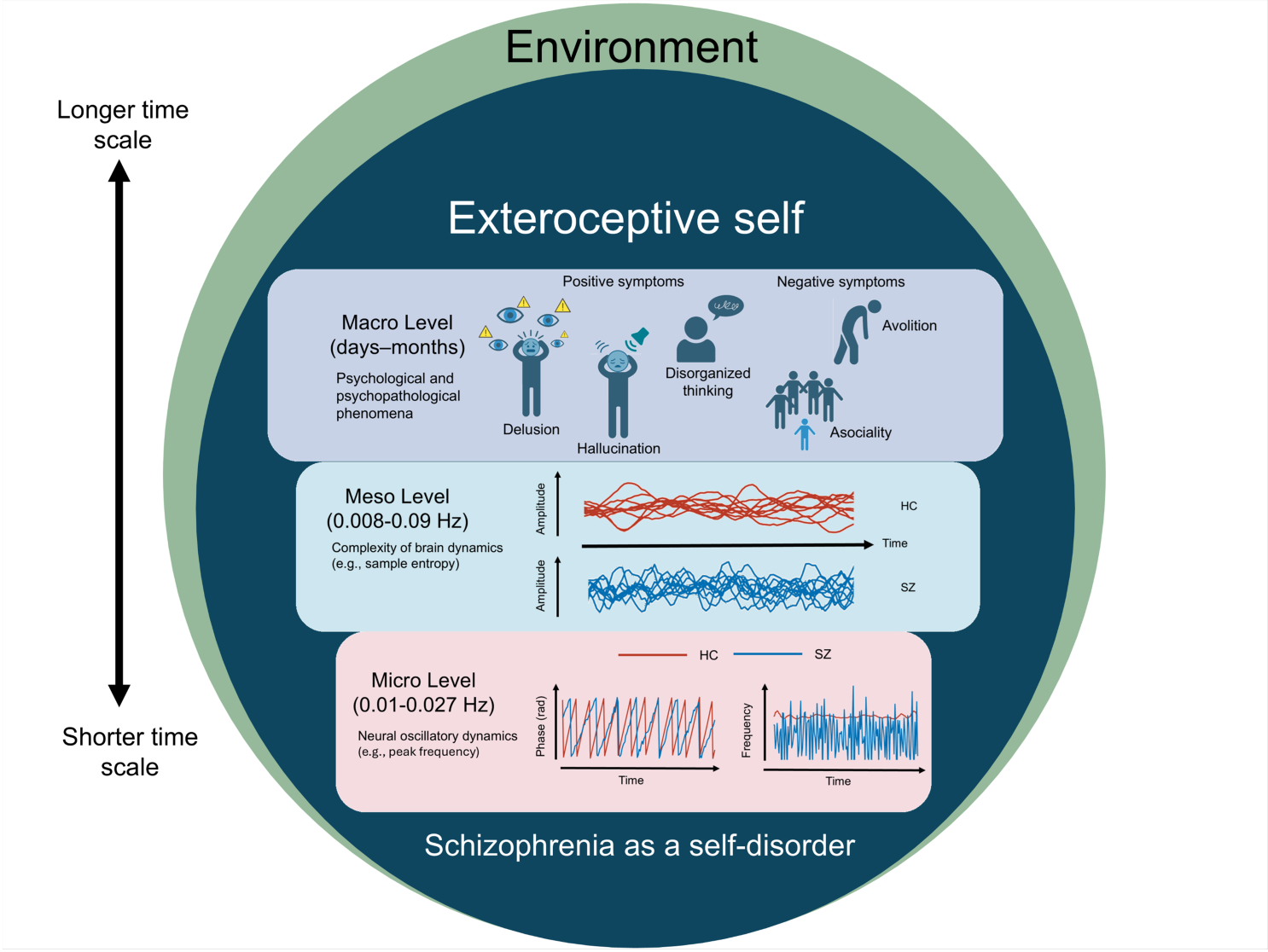


Figure 5

Multi-level framework of temporal imprecision in early psychosis. Temporal abnormalities in drug-free early psychosis are illustrated across three nested levels. Micro-level: infraslow neural oscillatory dynamics (0.01–0.027 Hz). Meso-level: complexity of brain dynamics measured by sample entropy (0.008–0.09 Hz). Macro-level: psychological and psychopathological phenomena observed over days to months. These nested processes primarily affect the exteroceptive self and are embedded within environmental interactions (outer circle). The framework highlights how disrupted neural timing scales up to behavioral and clinical manifestations, illustrating schizophrenia as a disorder of the self.

Supplementary Files

This is a list of supplementary files associated with this preprint. Click to download.

- supplementarymaterialsTP.docx